Aging and reliability of quantum networks

Lisa T. Weinbrenner [1,*] Lina Vandré [1,2] Tim Coopmans [3] and Otfried Gühne [1]

[1]*Naturwissenschaftlich-Technische Fakultät, Universität Siegen, Walter-Flex-Straße 3, 57068 Siegen, Germany*
[2]*State Key Laboratory for Mesoscopic Physics, School of Physics and Frontiers Science Center for Nano-Optoelectronics, Peking University, Beijing 100871, China*
[3]*Leiden Institute of Advanced Computer Science, Leiden University, Leiden, 2333 CA, The Netherlands*

Quantum information science may lead to technological breakthroughs in computing, cryptography, and sensing. For the implementation of these tasks, however, complex devices with many components are needed and the quantum advantage may easily be spoiled by the failure of only a few parts. A paradigmatic example is quantum networks. There, not only do noise sources such as photon absorption or imperfect quantum memories lead to long waiting times and low fidelity, but also hardware components may break, leading to a dysfunctionality of the entire network. For the successful long-term deployment of quantum networks in the future, it is important to take such deterioration effects into consideration during the design phase. Using methods from reliability theory and the theory of aging, we develop an analytical approach for characterizing the functionality of networks under aging and repair mechanisms, also for nontrivial topologies. Combined with numerical simulations, our results allow us to optimize long-distance entanglement distribution under aging effects.

I. INTRODUCTION

Modern experimental science is based on complex technical devices for measuring and manipulating physical systems. Examples are the Large Hadron Collider for testing the limits of the standard model and the observatory LIGO for detecting gravitational waves. All these experimental setups consist of many different parts, which must be functional for the whole device to be operational. In quantum technologies, typical setups include quantum computers or quantum networks which consist of many smaller quantum systems. Not only are these constituents prone to decoherence and noise, but they may also fail completely. To overcome this, redundancy and quantum error correction can be used and there is a trade-off between the required redundancy and the quality of the elementary devices. This trade-off is also relevant for comparing different quantum computing platforms, such as solid-state systems with many qubits and relatively short coherence times with ion traps, which have fewer but long-lived qubits [1,2]. For the long-term success, developing different approaches towards quantum technologies is important, but an advanced theory for analyzing the pros and cons of different implementation strategies is needed.

Besides quantum computers, quantum networks are a central paradigm of quantum technologies [3,4]. The aim of these networks is to enable global quantum communication, but they are also useful for distributed sensing [5–7], clock synchronization [8], and blind quantum computation [9]. Consequently, there are many theoretical proposals for

robust and efficient networks, using techniques such as quantum repeaters [10–13], multiplexing [14–17], and advanced quantum state encodings [18–20]. In recent years, different building blocks of quantum networks have been experimentally demonstrated, such as quantum teleportation between non-neighboring nodes [21], satellite to ground communication [22], and multiplexing [23,24]. All these implementations are, apart from the ubiquitous noise and photon loss, subject to deteriorating effects: Devices may be defect from the beginning or get destroyed during the experiment. In practice, devices may also fail only temporarily, due to, for example, overheating. While noise and loss in networks have been discussed in detail and may be overcome by entanglement purification, error correction, and other heralded procedures [20], the effects of aging, breaking, and repairing of hardware components are rarely studied. The present literature closest to this topic focuses on the waiting times and quantum-state quality for the functionality of a chain [14,25–34], where temporary hardware failure and recovery are absent, or global success probabilities for networks [35,36], where the topological structure of a specific network is often not taken into account. For a full characterization of aging effects and reliability, three main difficulties arise. First, the devices are highly dependent on each other due to feedback loops. Second, the topologies of networks are inherently more complicated than simple repeater chains. Third, the temporary failures of single devices may lead to temporal dependences of the working probability and correlations in time.

The goal of this paper is twofold. First, we show how ideas and concepts from reliability theory [37–39], known from sociology and the theory of aging, can be applied to the analysis of quantum networks. Second, we develop an

*lisa.weinbrenner@uni-siegen.de

analytical theory for discussing temporary failure and repairing in quantum networks. In contrast to classical networks, where adding redundant hardware is cheap, current quantum hardware is fragile, so it is essential to have a complete understanding of the network behavior to find the optimal protocols for it. Our approach differs from network percolation theory [40–42] by focusing on the temporal failure and recovery and is in line with recent work on fabrication defects in planar quantum computers [43]. The presented methods lead to various results. First, depending on a given figure of merit for the entire network, we can specify which type and quantity of redundant devices like quantum memories and entanglement sources are needed. Second, we can characterize the temporal correlations of a quantum network depending on the failure and repairing of each single device. Third, our results lead to improved cutoff times for key-generation protocols performed on these networks. As a main example we use the suggested configuration for a real quantum network in the Netherlands [44], but our results are easily extendable to more complex topologies.

The article is structured as follows. First, we explain in Sec. II the necessary concepts of quantum networks and in Sec. III the theory of aging and reliability theory. In Sec. IV we then apply reliability theory to quantum networks in general and demonstrate this approach for two different network topologies. In Sec. V we introduce the concept of repairing components in quantum networks and in Sec. VI we analyze the temporal correlations of broken components via different correlation measures. In Sec. VII we use our results to obtain improvements for quantum protocols performed on two different topologies of imperfect quantum devices.

II. QUANTUM NETWORKS

It is the general aim of a quantum network to generate entanglement in two distinct, far apart stations. However, the loss probability when exchanging entangled particles through a glass fiber increases exponentially with the distance. Therefore, one can use the concept of a quantum repeater [10–12], where several intermediate repeater stations are built between the end stations (see Fig. 1). Entanglement is first created and stored between adjacent repeater stations and then converted to long-range entanglement via Bell measurements within the stations. This setup allows one to overcome the exponential loss scaling. More generally, a quantum network may consist of many nodes which are connected by edges in various ways, leading to a complicated topology.

In order to explain our main ideas, we first focus on a simple network, the so-called repeater chain, consisting of $M + 1$ nodes connected with M edges in a linear configuration (see also Fig. 1). We allow multiplexing within the edges, meaning that each edge consists of N physical connections. Each connection can be seen as a physical system, where entanglement may be established, e.g., a spatial or spectral mode of a fiber for photons. The concept of multiplexing was introduced to allow for higher entanglement generation rates [14].

Our main aim is to characterize at which times the network is functional if some devices or connections break down permanently or become dysfunctional for a certain time, e.g., due
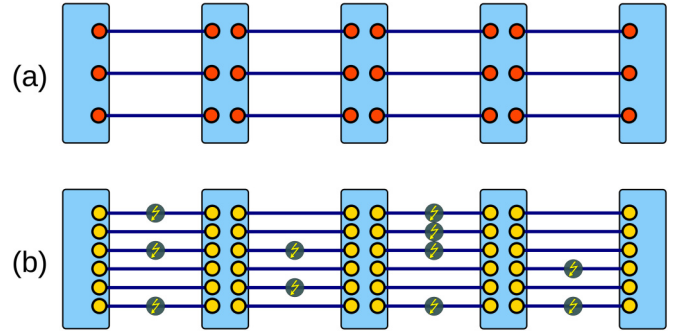

FIG. 1. (a) Schematic view of a multiplexed repeater chain, with $M + 1 = 5$ nodes and $M = 4$ edges, each edge having a multiplicity of $N = 3$. (b) Alternative approach for the implementation of a similar repeater chain, where initially $N = 6$ physical connections are established within the edges, but some of them are not functioning from the beginning. In this example, on average three physical connections are working. In the depicted example, there are two connections between the end nodes (as one edge contains only two working connections), so the flux of the entire chain is 2. Interestingly, both approaches, although being initially on average the same, can exhibit fundamentally different behavior on a long timescale.

to ice formation on a chip in a cryostat, overheating, or mechanical failures. So instead of describing the entanglement generation process and its timescales (as it has been done in Refs. [14,27,35], for example), we want to describe the functionality of the entire network depending on the functioning of each single device.

III. THEORY OF AGING

Biological and technical systems typically consist of many parts, with a complex structure of functional dependences. This raises the question of how long the entire system is functional, if some of the parts fail. The description of the reliability of such a complex system is the main goal of reliability theory [37,39]. The two main quantities are the reliability function

$$S(t) = \mathbb{P}(T > t), \tag{1}$$

which denotes the probability for a failure to occur at the failure time T after time t, so it describes the probability for the system to work at least until time t. This directly allows one to compute the mean time to failure via $\langle T \rangle = \int dt\, S(t)$. The failure rate

$$\mu(t) = -\frac{\partial_t S}{S} = -\partial_t \ln S(t) \tag{2}$$

describes the probability of a failure in the next time interval given the survival of the system until time t. Characteristic of the phenomenon of aging is the fact that the failure rate increases with time.

Starting from these two quantities, reliability theory offers a vast spectrum of results and algorithms. The reliability of a complicated system can be calculated, e.g., by a connection to repairable flow networks, for which many efficient algorithms are known [45]. Another main point in reliability theory is the effect of maintenance on the reliability of a system, considering pre-agreed strategies as well as adaptive strategies [46].

The starting point of our analysis arises from the suggestion of Gavrilov and Gavrilova to explain the different observed failure rates of technological devices [given by the Weibull power law $\mu(t) = at^b$ [47]] and biological systems [growing exponentially according to the Gompertz-Makeham law $\mu(t) = A + Be^{\lambda t}$ [48,49]] by using two different notions of redundancy (see Fig. 1). In technical systems (e.g., an aircraft), each subcomponent (e.g., the measurement devices of the air speed) appears in a fixed degree of redundancy and can be assumed to work in the beginning due to supervision and testing. In biological systems, however, the subcomponents (e.g., the organs) have a varying degree of redundancy, since some of their cells may not work right from the beginning. (See Ref. [50] for a criticism of the conclusions from these models in Refs. [38,51].)

IV. AGING THEORY FOR CHAINS AND NETWORKS

The methods from Ref. [38] can directly be extended to study the repeater chain. As implementation (a), corresponding to Fig. 1(a), we consider M edges with multiplicity N, working perfectly in the beginning, but affected by some failure rate μ, which describes the probability of a single edge to break down in the next time interval. As implementation (b), corresponding to Fig. 1(b), we consider the M edges connected with a higher multiplicity $N' > N$, where, however, with a certain probability $1 - p$, each connection is not working in the beginning. In practice, this may be caused by a lower quality of the devices, which are still favorable due to a lower price. In this case, the devices are affected by some failure rate μ'. For these two implementations, we are interested in the total number of parallel connections between the end nodes; this so-called flux corresponds to the minimum of the working connections taken over all edges. The flux describes the capacity for communication from one point to the other; it is therefore a crucial quantity in the real implementation of a network to analyze, e.g., the transmission delays for quantum communication [52,53]. Extending the methods from Ref. [38], any of the mentioned quantities can be fully determined analytically (details are given in Appendix A).

Naively, one may expect that the two implementations behave similarly, if $N'p = N$ and $\mu' = \mu$, that is, the number of initially working connections in the second implementation equals on average the number in the first implementation. This is however not the case. As a concrete example, we consider implementation (a) with $M = 6, N = 3$, and $\mu = 1/2$ and implementation (b) with $M = 6$, varying p, and varying μ'. Then we ask how large N' in implementation (b) needs to be such that implementation (b) has the same mean time to failure $\langle T \rangle$ as implementation (a). This is depicted as the blue surface in Fig. 2 and one finds that $N'p$ is typically significantly larger than N, even for $\mu' = \mu = 1/2$.

Furthermore, in implementation (b) it is not guaranteed at all that the chain works from the beginning. So we ask (for the same parameters) how large $N'p$ needs to be to guarantee that implementation (b) has in the beginning a working probability of at least $p_{\text{thres}} = 0.9$ (green surface in Fig. 2). Clearly, the lower the probability that a single connection is functioning, the higher the multiplicity needed for an initially working chain. Interestingly, for much lower failure rates $\mu' < \mu$ this
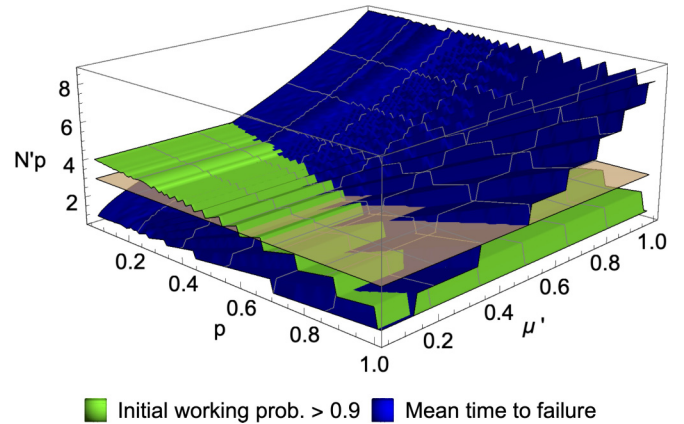

FIG. 2. Comparison between the implementations (a) and (b) (see Fig. 1) with respect to two different figures of merit: minimal multiplicity $N'p$ required in implementation (b) to reach the desired functionality in terms of lifetime and initial working probability as in implementation (a) with $N = 3$ and $\mu = 1/2$. The constant red half-transparent surface is given by $N'p = 3$. Note that the green surface given by the initial condition is constant with respect to μ'. The sawtoothlike pattern of steps is a direct consequence of the fact that N' is an integer number. See the text for more details.

is also the determining factor for N', if both conditions are to be satisfied. Hence we arrive at two different effects, relevant in different parameter regimes, that can be useful in determining which devices to consider when building a new network. Cheaper and imperfect devices with the same failure rate may seem tempting if the price of $N' = N/p$ devices compared to the price of N "perfect" devices is lower. However, as derived above, one actually needs a much higher number of cheaper devices than one would naively think.

While the repeater chain may be considered as a simple toy model, future quantum networks will have complex topologies [44]. Similarly, the components of other quantum technological devices are likely to exhibit more complicated functional dependences than the ones underlying the repeater chain. In order to demonstrate that our methods are capable of dealing with these, we consider a network as in Fig. 3(b), which can be seen as a structural approximation of an optimized network under realistic conditions [44]. In Appendix B we derive a formalism to deal with this type of topology using the method of indicator functions instead of probabilities.

We now demonstrate in some detail the methods described above on two different examples, one of them being the topology of Fig. 3. To summarize briefly, we see that there is a difference between the following two models.

(a) Each edge has a multiplicity of N, where every physical connection works perfectly in the beginning; however, the connections are affected by an exponential decay with failure rate μ.

(b) Each edge has a multiplicity of N', where each physical connection is not working in the beginning with a certain probability $1 - p$; the connections are also affected by an exponential decay with failure rate μ'.

In Fig. 4 we plot now the two resulting reliability functions and failure rates for these two models and two different topologies. The first topology is again a chain consisting of
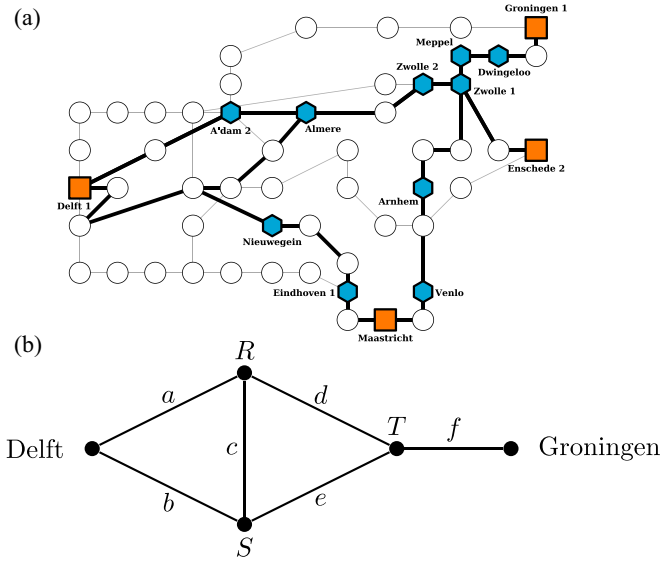
FIG. 3. (a) Optimized network topology for a network relying on the the Dutch telecom infrastructure (figure taken from Ref. [44]). (b) Structural approximation of this network for a connection from Delft to Groningen. This network consists of five nodes and six connections.

$M = 6$ edges, compared to the simplified topology of the network in Fig. 3, which also consists of six edges. The results for the network are obtained using indicator functions as described in Appendix B. There are several observations. First, the reliability functions according to model (b) have a negative offset at $t = 0$. This should be expected, as there is a nonzero probability that the whole system is not functional right from the start as each connection is only functional with probability p. However, the offset is smaller in the case of the network since there are more possible end-to-end paths. Analogously, the failure rates for model (b) do not start at 0 for $t = 0$. A second observation shows that the two models behave the same in the long run. If the individual connections start to fail, then at some point one cannot distinguish anymore between an initially broken connection and a connection which just broke in the last few seconds. However, in the short time range model (a) performs better. The last observation concerns the different topologies. It is not surprising that the network shows a more stable behavior, that is, a slower decreasing reliability and a slower increasing failure rate. The chain will fail as soon as one of the edges fails; the network, however, is robust to the failure of up to three edges as long as a path still exists from end to end.

V. REPAIRING COMPONENTS IN NETWORKS

Here we consider multiplexed networks or repeater chains, where the physical connections may break down according to the models discussed above, but broken connections can be repaired. We assume that the repairing process takes several time steps.

Several questions can be asked in this situation. The first one concerns the probability that, at a given point in time, the network is functional. Second, one can ask for the probability
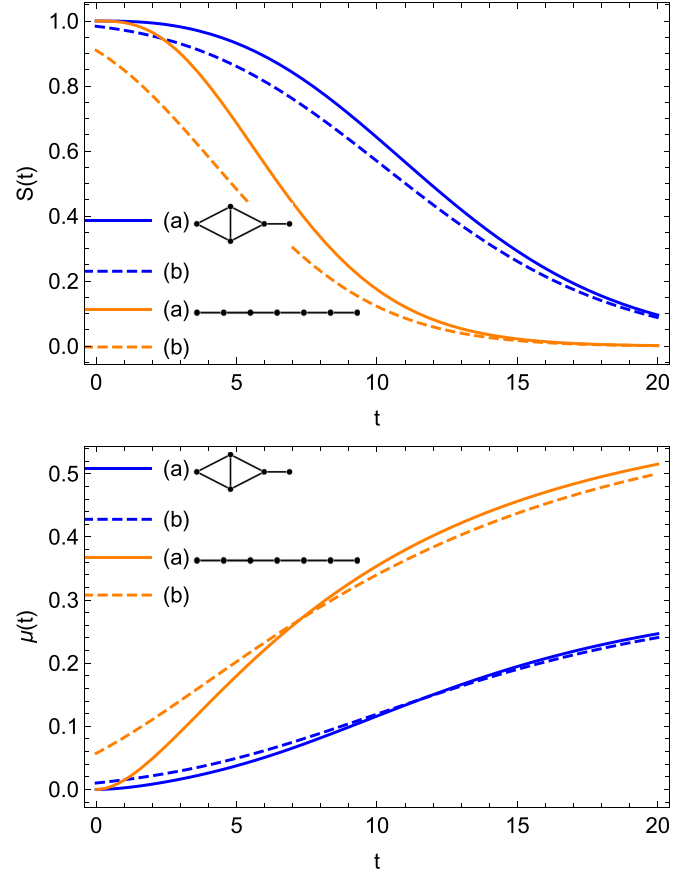

FIG. 4. Reliability function $S(t)$ and failure rate $\mu(t)$ of a network [blue (dark gray)] or chain [orange (light gray)] depending on the time t, both consisting of six edges; the solid lines denote the results for model (a), where each edge has a multiplicity of $N = 3$, and the dashed lines denote the results for model (b), where each edge has a multiplicity of $N' = 6$ and an initial failure probability of $1 - p = 1/2$. For the description of the models see Fig. 1 and Sec. IV.

that the entire network is broken for several consecutive time steps. Formally, this is related to the calculation of waiting times for entanglement generation in networks with finite memory [14,26] and is challenging due to the complicated temporal dependences of the model. In the following, however, we will develop a method to tackle this.

We use for our calculations the following discrete instead of continuous model. Each connection can break in a single time step with constant probability $p_\downarrow$, so the breaking of the connection is geometrically distributed, which can be seen as the discrete analog of the exponential distribution with the mean value $1/p_\downarrow$. If the connection now breaks, it remains nonfunctional for exactly τ time steps, where τ is a constant set in advance. After this, it is functional with probability $1 - p_\downarrow$, but with probability $p_\downarrow$ it breaks directly again, leaving it broken for at least 2τ consecutive time steps.

Since the expectation value of a geometric distribution is given by $1/p_\downarrow$, the connection is on average functional for $1/p_\downarrow - 1$ time steps before breaking. The connection is thus broken on τ out of on average $1/p_\downarrow - 1 + \tau$ time steps, so the average probability of a single connection to be broken is
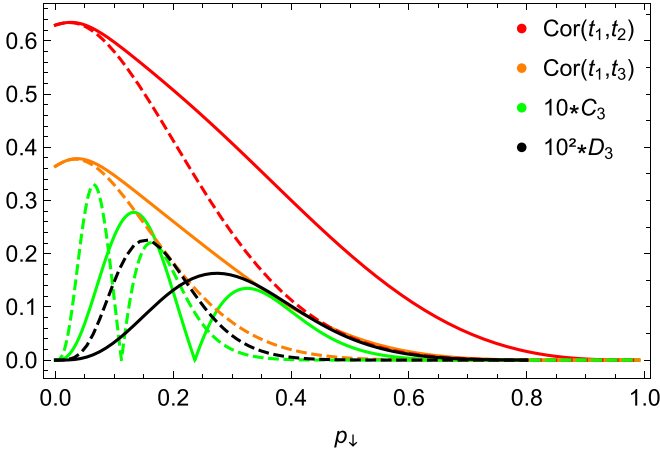
FIG. 5. Four different correlation measures demonstrating the dependences in the temporal behavior of two network models. Solid lines show the results for the network in Fig. 3 and the dashed lines show results for a repeater chain similar to Fig. 1(a) with $M = 6$ connections. Both network structures have a multiplicity of $N = 3$ and a repairing time of $\tau = 7$.

given by $\tau/(1/p_\downarrow - 1 + \tau)$. For a repeater chain with M edges of multiplicity N this leads to an average working probability of

$$q = \left[1 - \left(\frac{\tau}{\frac{1}{p_\downarrow} - 1 + \tau} \right)^N \right]^M. \tag{3}$$

By using more subtle counting arguments we can also calculate the probability that a chain or network displays a certain behavior in t consecutive but arbitrarily chosen time steps. For the exact calculations we refer the reader to Appendix C. Our results can be used to characterize the time dependences of the system and in particular to calculate the probability for a given network to be functional conditioned on the time step(s) before.

VI. CORRELATION MEASURES

Here we give an example how the results described above can be used to analyze the temporal correlations in various network structures. In Fig. 5 we present in detail the behavior in up to three consecutive time steps of a multiplexed network and a multiplexed repeater chain with repairing. The chain consists again of $M = 6$ edges, and for both topologies we have a multiplicity of $N = 3$ and a repairing time of $\tau = 7$. The total state of each of the networks can assume two values, $S = 0$ for not working and $S = 1$ for working. The analytical results (see Appendix C) for this random variable allow one to calculate various correlations at different times.

We first consider the normalized temporal correlation

$$\text{Cor}(t_a, t_b) = \frac{\langle S(t_a)S(t_b) \rangle - \langle S(t_a) \rangle \langle S(t_b) \rangle}{\sigma(S(t_a))\sigma(S(t_b))} \tag{4}$$

for two consecutive time steps t_1 and t_2 or with one time step in between t_1 and t_3, where $\sigma(S(t_x))$ denotes the standard deviation. Then we consider two established measures of genuine tripartite correlation. The first one is the joint cumulant C_3

[54], which for three random variables A, B, and C is defined as

$$C_3 = |\langle ABC \rangle - \langle A \rangle \langle BC \rangle - \langle B \rangle \langle AC \rangle - \langle C \rangle \langle AB \rangle$$
$$+ 2\langle A \rangle \langle B \rangle \langle C \rangle|.$$

If the joint cumulant is nonzero, then none of the three random variables is independent of the other two. However, the other direction does not always hold.

The second measure D_3 of tripartite correlations is based on exponential families and an extension of the multi-information, which is used in the analysis of complex systems [55–57]. The Kullback-Leibler distance

$$D(P||Q) = \sum_j p_j \log_2(p_j/q_j) \tag{5}$$

describes how surprising the probability distribution P is if one had expected the distribution Q. Then the correlation measure D_3 of a three-variable distribution is given by the minimal distance to all probability distributions $Q \in \mathcal{E}_2$ which are thermal states of two-body Hamiltonians, that is,

$$D_3(P) = \inf_{Q \in \mathcal{E}_2} D(P||Q).$$

This describes genuine three-party correlations and is used in the analysis of complex systems [55].

Looking at the results in Fig. 5, the first observation is that the repeater chain shows high time dependences for smaller breaking probabilities $p_\downarrow$ than the network. This is somewhat intuitive: If a complete failure of a system rarely but at least sometimes happens, then it is more probable that the system is broken for a few time steps in sequence than in randomly chosen time steps, leading to high time dependences. Since the network is more robust to breaking, this behavior occurs for the network for higher breaking probabilities. Second, the joint cumulant C_3 tends to zero if the system is equally often broken as functional. Around this point the correlation measure D_3 reaches its maximum. Third, every correlation measure tends to 0 for high $p_\downarrow$, since in that case the systems remain broken most of the time.

VII. APPLICATIONS IN ENTANGLEMENT DISTRIBUTION

Now we use our results to derive improvements for quantum protocols run on these setups. We consider entanglement generation and subsequent quantum key distribution with quantum repeaters as described above. One problem in these schemes is that the quality of existing entangled links decreases when stored, due to decoherence. These weakly entangled links do not lead to high-fidelity long-range entanglement anymore and block the generation of fresh entangled pairs, so it may be useful to restrict the duration of an entanglement generation attempt by a cutoff time and erase all created links after this time [14,58]. The cutoff time should be chosen in such a way that the secret-key rate achieved by this protocol is optimal [28,32,59].

We aim to find a strategy for optimizing the cutoff time for the network in Fig. 3 without multiplexing and for a chain of $M = 6$ edges with multiplicity $N = 3$. We assume two different timescales: On the longer timescale devices break and are repaired; on top of that and on a much shorter timescale,
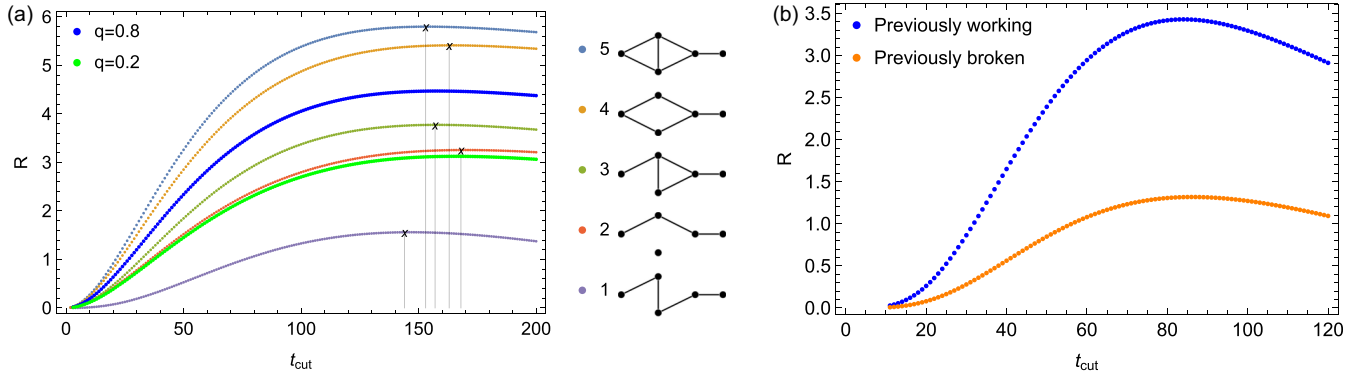
FIG. 6. Secret-key rate (bits per second) (a) in the simplified Netherlands network with $N = 1$ and (b) on a chain with $M = 6$ edges with $N = 3$, depending on the chosen cutoff time. See the text for more details.

entanglement is probabilistically distributed according to the protocol above. For the secret-key rates we now simulate the repeater protocol, assuming perfect Bell measurements and a entanglement generation probability of $P_{\text{gen}} = 0.01$. Decoherence is modeled as depolarizing noise with a coherence time of $T_{\text{coh}} = 1$ s and the duration of one time step for the quantum protocol is $\frac{2}{3} \times 10^{-3}$ s. (For the motivation for these numbers and more details, see Ref. [60] and Appendix D.)

The results of our simulations are shown in Fig. 6. In Fig. 6(a) the thin lines denote the secret-key rates achieved on the five different configurations of the Netherlands network depending on the chosen cutoff time. Assuming that a single edge of the network has an average working probability of $q = 0.8$ or 0.2, one can calculate the probabilities for the network to be in a certain configuration and from this the average secret-key rate achieved on the network. Clearly, these average key rates are lower than the one achieved on the complete network, so the classical defects of the technical devices have a significant impact on the quantum efficiency. A second observation is that the secret-key rate reaches a different maximum for each configuration, with the largest distance between two maxima given by $\Delta t_{\text{cut}} = t_{\text{cut,2}} - t_{\text{cut,1}} = 168 - 144 = 24$, corresponding to a relative change from configuration 1 to configuration 2 of around 17%. So knowing the characteristics of the technical devices leads to a better choice of the cutoff time.

In the same way as above, we simulated the achievable key rates on a repeater chain with $M = 6$ edges with multiplicity $N = 3$. For the breaking probability we chose $p_{\downarrow} = 1/105$ and for the repairing time $s = 15$. The resulting average key rates can be seen in Fig. 6(b). Here we took the state of the repeater chain in the previous time step into consideration and conditioned the probabilities for the different functional configurations on whether the repeater chain was functional or broken in the previous step. One can see a clear difference between the key rates in these two different cases, which is to be expected. If the chain was functional in the time step before, then the configurations with a higher multiplicity in the edges are more probable than if the chain was broken in the previous step. So the knowledge about the previous behavior of the repeater chain can be used to choose an appropriate cutoff time for the current experiment and the breaking effects of the used technical devices can be mitigated by adapting the cutoff time of the quantum protocol to the current situation.

VIII. CONCLUSION

We developed analytical methods to treat failure and defects of classical devices in quantum networks and which can be used to study temporal correlations arising from failure-and-repair mechanisms. Based on our results, we showed that these classical effects have an impact on the performed quantum protocol and give rise to new criteria for an optimal cutoff time in repeater protocols. Our methods are also directly applicable to recent experimental implementations. One example is the four-party network implemented in [61], where different errors in the state generation or in the experimental equipment can directly be translated to failures of nodes or edges in our framework. Our methodology can also be applied to give additional constraints for developing new repeater architectures as in [62], where a potentially multiplexed repeater chain is considered.

While our methods were developed in the quantum network paradigm, it seems promising to adapt them to other examples of quantum technologies. A concrete example is segmented ion traps [63,64]. Here ions are shuttled on a chip from one interaction zone to the other to build quantum circuits with high fidelity. Failures of interaction or shuttling procedures can directly be modeled with our approach and consequently the design of these ion traps can be optimized. On a more fundamental level, our results can be used to optimize entanglement distribution in networks [36,65] as well as multipartite cryptographic protocols [66]. Finally, it would be interesting to exploit the further results and methods from reliability theory [45,46,67,68] to today's quantum technologies.

The code can be found online [69]. The computed data can be made available upon reasonable request.

APPENDIX A: RELIABILITY THEORY FOR REPEATER CHAINS

In this Appendix we describe how one can apply reliability theory to repeater chains. First, we give a short introduction to the basics of reliability theory and the main quantities. Second, we derive some results for the easiest network structure, the repeater chain. We start by considering a single connection and then an edge or block, which consists of N parallel connections. Here we differentiate between a block consisting of N initially perfect connections and N connections which may be broken in the beginning with probability $1 - p$. Finally, these blocks of connections are combined into a chain. All the results are purely analytical.

1. Basics of reliability theory

The reliability function $S(t)$ describes the probability that a system fails after a certain time t and is functional up to this point. If T is the random variable describing the failure time of the system then

$$S(t) = \mathbb{P}(T > t). \tag{A1}$$

Using the cumulative distribution function

$$F(t) = \mathbb{P}(T \leqslant t), \tag{A2}$$

one can express the reliability function as

$$S(t) = 1 - \mathbb{P}(T \leqslant t) = 1 - F(t). \tag{A3}$$

The failure rate of the system is given by the logarithmic derivative of the reliability function

$$\mu(t) = -\frac{\mathrm{d}}{\mathrm{d}t} \ln S(t) = -\frac{1}{S(t)} \frac{\mathrm{d}}{\mathrm{d}t} S(t) = \frac{1}{S(t)} \frac{\mathrm{d}}{\mathrm{d}t} F(t). \tag{A4}$$

Sometimes it is easier to express the failure rate using the probability density function

$$f(t) = \frac{\mathrm{d}}{\mathrm{d}t} F(t) = -\frac{\mathrm{d}}{\mathrm{d}t} S(t). \tag{A5}$$

It then holds that

$$\mu(t) = \frac{f(t)}{S(t)}. \tag{A6}$$

2. Results for repeater chains

One block consists of a fixed number of N parallel connections. Each of these connections can be functional or broken. The block has a flux of $\mathfrak{f}$ if at least $\mathfrak{f}$ of the N connections are functional. We want to calculate the probability to have a certain flux $\mathfrak{f}$ depending on the time t. The calculation follows the strategy of Gavrilov and Gavrilova [38], with some modifications to avoid the underlying implicit assumption of small timescales (see also Ref. [50]). The important difference is that in their calculations a block fails if all connections are destroyed. In our calculation the block "fails" if $N - (\mathfrak{f} - 1)$ connections are destroyed, because then a flux of $\mathfrak{f}$ is not possible anymore.

a. Single connection

A single connection has a fixed failure rate $\mu(t) = k = \mathrm{const}$, so it decays exponentially. Let T be the random variable which describes the failure time of a single connection. For the exponential distribution it holds that

$$S(1, k, t) := \mathbb{P}(T > t) = 1 - F(t) = e^{-kt} =: \alpha \tag{A7}$$

and

$$F(1, k, t) := \mathbb{P}(T \leqslant t) = 1 - e^{-kt} = 1 - \alpha. \tag{A8}$$

Note that the following holds:

$$\frac{\mathrm{d}\alpha}{\mathrm{d}t} = -ke^{-kt} = -k\alpha. \tag{A9}$$

b. Block with initially perfect connections

One block consists of a fixed number of connections N. In the beginning all N of these connections are functional. We want to calculate the probability to have a certain flux $\mathfrak{f}$ depending on the time t.

Proposition 1. Given a block of N working connections which each fail according to a constant failure rate $\mu(t) = k$, the reliability function of the block b for a flux $\mathfrak{f}$ at time t is given by

$$S_b^{\mathfrak{f}}(N, k, t) = \sum_{i=0}^{N-\mathfrak{f}} \binom{N}{i}(1 - \alpha)^i \alpha^{N-i} \tag{A10}$$

and the failure rate is given by

$$\mu_b^{\mathfrak{f}}(N, k, t) = \frac{k\mathfrak{f}\binom{N}{\mathfrak{f}}(1 - \alpha)^{N-\mathfrak{f}}\alpha^{\mathfrak{f}}}{\sum_{i=0}^{N-\mathfrak{f}} \binom{N}{i}(1 - \alpha)^i \alpha^{N-i}} \tag{A11}$$

with $\alpha = e^{-kt}$.

Proof. Denote the failure time of the block by T_b and the failure time of the ith connection by T_i. The failure times of the connections are independent and identically distributed, so the probability for the failure of i arbitrary connections is the same as for the connections $1, \ldots, i$. The block fails in time $T_b \leqslant t$ and therefore has a flux less than or equal to $\mathfrak{f} - 1$, if at least $N - (\mathfrak{f} - 1)$ of the connections fail before t:

$$
\begin{aligned}
F_b^{\mathfrak{f}}(N, k, t) &= \mathbb{P}(T_b \leqslant t) \\
&= \sum_{i=N-(\mathfrak{f}-1)}^{N} \binom{N}{i} \mathbb{P}(T_1, \ldots, T_i \leqslant t) \\
&\quad \times \mathbb{P}(T_{i+1}, \ldots, T_N > t) \\
&= \sum_{i=N-(\mathfrak{f}-1)}^{N} \binom{N}{i} \mathbb{P}(T_1 \leqslant t) \cdots \mathbb{P}(T_i \leqslant t) \\
&\quad \times \mathbb{P}(T_{i+1} > t) \cdots \mathbb{P}(T_N > t) \\
&= \sum_{i=N-(\mathfrak{f}-1)}^{N} \binom{N}{i} [F(1, k, t)]^i [S(1, k, t)]^{N-i} \\
&= \sum_{i=N-(\mathfrak{f}-1)}^{N} \binom{N}{i} (1 - \alpha)^i \alpha^{N-i}
\end{aligned}
$$

$$= \sum_{i=0}^{N} \binom{N}{i}(1-\alpha)^i \alpha^{N-i} - \sum_{i=0}^{N-\mathfrak{f}} \binom{N}{i}(1-\alpha)^i \alpha^{N-i}$$

$$= 1 - \sum_{i=0}^{N-\mathfrak{f}} \binom{N}{i}(1-\alpha)^i \alpha^{N-i}. \tag{A12}$$

The reliability function is then given by

$$S_b^{\mathfrak{f}}(N,k,t) = \mathbb{P}(T_b > t) = 1 - F_b^{\mathfrak{f}}(N,k,t)$$

$$= \sum_{i=0}^{N-\mathfrak{f}} \binom{N}{i}(1-\alpha)^i \alpha^{N-i}. \tag{A13}$$

For the failure rate we calculate first the probability density function

$$f_b^{\mathfrak{f}}(N,k,t) = -\frac{\mathrm{d}}{\mathrm{d}t} S_b^{\mathfrak{f}}(N,k,t) \tag{A14}$$

$$= -\frac{\mathrm{d}\alpha}{\mathrm{d}t}\frac{\mathrm{d}}{\mathrm{d}\alpha} \sum_{i=0}^{N-\mathfrak{f}} \binom{N}{i}(1-\alpha)^i \alpha^{N-i}$$

$$= k\alpha \left[\sum_{i=0}^{N-\mathfrak{f}} \binom{N}{i}(1-\alpha)^i (N-i)\alpha^{N-i-1} + \sum_{i=1}^{N-\mathfrak{f}} \binom{N}{i}(-1)i(1-\alpha)^{i-1}\alpha^{N-i} \right]$$

$$= k\alpha \left[\sum_{i=0}^{N-\mathfrak{f}} \binom{N}{i}(N-i)(1-\alpha)^i \alpha^{N-i-1} - \sum_{i=0}^{N-\mathfrak{f}-1} \binom{N}{i+1}(i+1)(1-\alpha)^i \alpha^{N-(i+1)} \right]. \tag{A15}$$

Then it holds that

$$\binom{N}{i+1}(i+1) = \frac{N!}{(i+1)!(N-i-1)!}(i+1) = \frac{N!}{i!(N-i)!}(N-i) = \binom{N}{i}(N-i) \tag{A16}$$

and therefore

$$f_b^{\mathfrak{f}}(N,k,t) = k\alpha \left[\sum_{i=0}^{N-\mathfrak{f}} \binom{N}{i}(N-i)(1-\alpha)^i \alpha^{N-i-1} - \sum_{i=0}^{N-\mathfrak{f}-1} \binom{N}{i}(N-i)(1-\alpha)^i \alpha^{N-(i+1)} \right]$$

$$= k\alpha \binom{N}{N-\mathfrak{f}}[N-(N-\mathfrak{f})](1-\alpha)^{N-\mathfrak{f}}\alpha^{\mathfrak{f}-1}$$

$$= k\mathfrak{f}\binom{N}{\mathfrak{f}}(1-\alpha)^{N-\mathfrak{f}}\alpha^{\mathfrak{f}}. \tag{A17}$$

The failure rate is then the fraction of the probability density function and the reliability:

$$\mu_b^{\mathfrak{f}}(N,k,t) = \frac{f_b^{\mathfrak{f}}(N,k,t)}{S_b^{\mathfrak{f}}(N,k,t)}$$

$$= \frac{k\mathfrak{f}\binom{N}{\mathfrak{f}}(1-\alpha)^{N-\mathfrak{f}}\alpha^{\mathfrak{f}}}{\sum_{i=0}^{N-\mathfrak{f}} \binom{N}{i}(1-\alpha)^i \alpha^{N-i}}$$

$$= \frac{k\mathfrak{f}\binom{N}{\mathfrak{f}}(\alpha^{-1}-1)^{N-\mathfrak{f}}}{\sum_{i=0}^{N-\mathfrak{f}} \binom{N}{i}(\alpha^{-1}-1)^i}. \tag{A18}$$

∎

c. Block with probabilistic connections

In this model one block consists of a fixed number of connections N. In the beginning, only n of these connections are functional. The number n depends on some probability distribution q_n with $\sum_{n=0}^{N} q_n = 1$, e.g., the binomial distribution $q_n = \binom{N}{n}p^n(1-p)^{N-n}$. The binomial distribution describes the case where each single connection is functional with probability p. In general, the distribution q_n can be arbitrary.

We want to calculate the probability to have a certain flux $\mathfrak{f}$ depending on the time t.

Proposition 2. Given a block of N connections of which n connections are working in the beginning with probability q_n and denote the probability distribution by $Q = \{q_n\}$. Each working connection fails according to a constant failure rate $\mu(t) = k$. Then the reliability function of the block for a flux $\mathfrak{f}$ at time t is given by

$$S_b^{\mathfrak{f}}(N,Q;k,t) = \sum_{n=\mathfrak{f}}^{N} q_n S_b^{\mathfrak{f}}(n,k,t) \tag{A19}$$

and the failure rate is given by

$$\mu_b^{\mathfrak{f}}(N,Q;k,t) = \frac{1}{S_b^{\mathfrak{f}}(N,Q;k,t)} \sum_{n=\mathfrak{f}}^{N} q_n \mu_b^{\mathfrak{f}}(n,k,t) S_b^{\mathfrak{f}}(n,k,t). \tag{A20}$$

Proof. Using the law of total probability, it holds for the reliability that

$$S_b^{\mathfrak{f}}(N,Q;k,t) = \mathbb{P}(T_b > t) = \sum_{n=\mathfrak{f}}^{N} q_n S_b^{\mathfrak{f}}(n,k,t). \tag{A21}$$

For the failure rate it then follows that

$$
\mu_b^{\mathfrak{f}}(N, Q; k, t) = -\frac{1}{S_b^{\mathfrak{f}}(N, Q; k, t)} \frac{\mathrm{d}}{\mathrm{d}t} \sum_{n=\mathfrak{f}}^{N} q_n S_b^{\mathfrak{f}}(n, k, t)
$$

$$
= \frac{1}{S_b^{\mathfrak{f}}(N, Q; k, t)} \sum_{n=\mathfrak{f}}^{N} q_n S_b^{\mathfrak{f}}(n, k, t)
$$

$$
\times \left(-\frac{1}{S_b^{\mathfrak{f}}(n, k, t)} \frac{\mathrm{d}}{\mathrm{d}t} S_b^{\mathfrak{f}}(n, k, t) \right)
$$

$$
= \frac{1}{S_b^{\mathfrak{f}}(N, Q; k, t)} \sum_{n=\mathfrak{f}}^{N} q_n S_b^{\mathfrak{f}}(n, k, t) \mu_b^{\mathfrak{f}}(n, k, t). \tag{A22}
$$

∎

In Ref. [38] they use at this point implicitly an approximation for small timescales by calculating the failure rate for a flux of $\mathfrak{f} = 1$ without the weights $\frac{S_b^1(n, k, t)}{S_b^1(N, Q; k, t)}$:

$$
\mu_b^1(N, Q; k, t) = \sum_{n=1}^{N} \tilde{q}_n \mu_b^1(n, k, t). \tag{A23}
$$

The probabilities $\tilde{q}_n$ are normalized such that the probability $\tilde{q}_0$ for a failure right in the beginning is 0. In this case, the reliabilities $S_b^1(N, Q; k, 0) = 1$ and $S_b^1(n, k, 0) = 1$ cancel for $t = 0$ (since the device is surely functional in the beginning). However, for larger times t the weights become relevant and lead to a very different behavior than in Ref. [38].

d. Chain

Proposition 3. Given a chain of M blocks with respective reliability functions $S_{b_j}(t)$ and failure rates $\mu_{b_j}(t)$, $j = 1, \dots, M$, the reliability function and failure rate of the whole chain are given by the product or sum, respectively:

$$
S_{\mathrm{chain}} = \prod_{j=1}^{M} S_{b_j}(t), \quad \mu_{\mathrm{chain}}(t) = \sum_{j=1}^{M} \mu_{b_j}(t). \tag{A24}
$$

Proof. Let T_{chain} be the failure time of the chain and T_{b_j} the failure time of block $j = 1, \dots, M$. The failure times of the blocks are independent but not necessarily identically distributed. The whole chain fails if at least one of the blocks fails. Therefore, it holds that

$$
S_{\mathrm{chain}}(t) = \mathbb{P}(T_{\mathrm{chain}} > t) = \mathbb{P}(T_{b_1}, \dots, T_{b_M} > t)
$$

$$
= \prod_{j=1}^{M} \mathbb{P}(T_{b_j} > t) = \prod_{j=1}^{M} S_{b_j}(t) \tag{A25}
$$

and

$$
\mu_{\mathrm{chain}}(t) = -\frac{\mathrm{d}}{\mathrm{d}t} \ln S_{\mathrm{chain}}(t) = -\frac{\mathrm{d}}{\mathrm{d}t} \ln \prod_{j=1}^{M} S_{b_j}(t)
$$

$$
= \sum_{j=1}^{M} \left(-\frac{\mathrm{d}}{\mathrm{d}t} \ln S_{b_j}(t) \right) = \sum_{j=1}^{M} \mu_{b_j}(t). \tag{A26}
$$

∎

If the blocks are all independent and identically distributed, then it simply holds that

$$
S_{\mathrm{chain}}(t) = [S_b(t)]^M \tag{A27}
$$

and

$$
\mu_{\mathrm{chain}}(t) = M \mu_b(t). \tag{A28}
$$

APPENDIX B: PROBABILITIES IN MORE COMPLEX TOPOLOGIES

To calculate the probabilities for a network to be functional or not, one has to consider the different possible paths in this network that lead to a resulting connection from one point of the network to another. This type of probability can be computed, e.g., using the principle of inclusion and exclusion. Another easier and more clear option is the use of indicator functions. This idea can be found in, e.g., Ref. [70]. We use indicator functions of the type

$$
\mathbb{1}_X = \begin{cases} 1 & \text{if } X \text{ is functional} \\ 0 & \text{if } X \text{ is broken.} \end{cases} \tag{B1}
$$

Then it holds that

$$
\mathbb{E}[\mathbb{1}_X] = 1 \times \mathbb{P}(X \text{ is functional}) + 0 \times \mathbb{P}(X \text{ is broken})
$$

$$
= \mathbb{P}(X \text{ is functional}). \tag{B2}
$$

So to calculate the probability for the whole system to be functional we first calculate the indicator function and then take the average value.

If A and B are two components, which are connected in series to get the larger component X, then X is functional if and only if A and B are functional. The indicator function of X then reads

$$
\mathbb{1}_X = \begin{cases} 1 & \text{if } \mathbb{1}_A = \mathbb{1}_B = 1 \\ 0 & \text{otherwise} \end{cases}
$$

$$
= \mathbb{1}_A \times \mathbb{1}_B \tag{B3}
$$

and the probability is therefore (since A and B are independent)

$$
\mathbb{P}(X \text{ is functional}) = \mathbb{E}[\mathbb{1}_X] = \mathbb{E}[\mathbb{1}_A] \times \mathbb{E}[\mathbb{1}_B]
$$

$$
= \mathbb{P}(A \text{ is functional}) \times \mathbb{P}(B \text{ is functional}). \tag{B4}
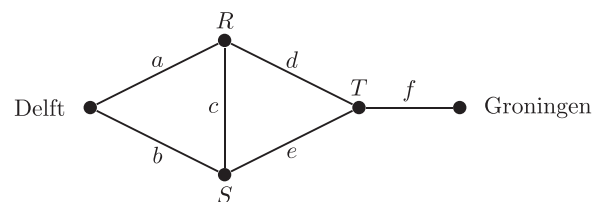$$

FIG. 7. Simplification of the network in Ref. [44] from Delft to Groningen. The network consists of three components in series: a square network (with one diagonal connection c) from Delft up to node T, the node T itself, and a single connection f to Groningen.

If the components are connected in parallel, the indicator function of X instead reads

$$\mathbb{1}_X = \begin{cases} 1 & \text{if } \mathbb{1}_A = 1 \text{ or } \mathbb{1}_B = 1 \\ 0 & \text{otherwise} \end{cases} = 1 - (1 - \mathbb{1}_A) \times (1 - \mathbb{1}_B) \tag{B5}$$

and the probability is (since A and B are independent)

$$\mathbb{P}(X \text{ is functional}) = \mathbb{E}[\mathbb{1}_X] = 1 - (1 - \mathbb{E}[\mathbb{1}_A]) \times (1 - \mathbb{E}[\mathbb{1}_B]) = 1 - \mathbb{P}(A \text{ is broken}) \times \mathbb{P}(B \text{ is broken}). \tag{B6}$$

The idea to use indicator functions instead of probabilities becomes more interesting when considering more difficult networks. For the simple square network with one diagonal connection (see Fig. 7, where the square contains the connections from Delft to the node T, including nodes R and S) the indicator function becomes

$$\mathbb{1}_{\text{square}} = \begin{cases} 1 & \text{if } \mathbb{1}_{aRd} = 1 \text{ or } \mathbb{1}_{aRcSe} = 1 \text{ or } \mathbb{1}_{bSe} = 1 \text{ or } \mathbb{1}_{bScRd} = 1 \\ 0 & \text{otherwise} \end{cases}$$

$$= 1 - (1 - \mathbb{1}_{aRd}) \times (1 - \mathbb{1}_{aRcSe}) \times (1 - \mathbb{1}_{bSe}) \times (1 - \mathbb{1}_{bScRd}), \tag{B7}$$

where $\mathbb{1}_{aRd}$ is the short notation for $\mathbb{1}_a \mathbb{1}_R \mathbb{1}_d$. Using the fact that $\mathbb{1}^2 = \mathbb{1}$, one obtains

$$\mathbb{1}_{\text{square}} = \mathbb{1}_{aR}(\mathbb{1}_d + \mathbb{1}_{cSe} - \mathbb{1}_{decS})$$
$$+ \mathbb{1}_{bS}(\mathbb{1}_e + \mathbb{1}_{cRd} - \mathbb{1}_{ecdR})$$
$$- \mathbb{1}_{abRS}(\mathbb{1}_{de} + \mathbb{1}_{cd} + \mathbb{1}_{ce} - 2 \times \mathbb{1}_{ced}). \tag{B8}$$

Note that all the indicator functions in the products are independent. Therefore, one can just calculate the average value of each single term to get the average value of $\mathbb{1}_{\text{square}}$. In the special case that the edges and nodes all have the same respective probabilities for failures $\mathbb{P}(\text{edge is broken}) = 1 - e$ and $\mathbb{P}(\text{node is broken}) = 1 - n$, the probability for the network to be functional is simply

$$\mathbb{P}(\text{square is functional})$$
$$= \mathbb{E}[\mathbb{1}_{\text{square}}]$$
$$= en(e + e^2n - e^3n) + en(e + e^2n - e^3n)$$
$$- e^2n^2(e^2 + e^2 + e^2 - 2 \times e^3)$$
$$= 2e^2n + e^3n^2(2 - 5e + 2e^2). \tag{B9}$$

The network in Ref. [44] from Delft to Groningen is then a series of a square network, a node T, and a single connection f. Therefore, the indicator function for the connection from Delft to Groningen reads

$$\mathbb{1}_X = \mathbb{1}_{\text{square}} \times \mathbb{1}_T \times \mathbb{1}_f. \tag{B10}$$

APPENDIX C: REPAIRING BROKEN DEVICES AND RESULTING NON-MARKOVIAN EFFECTS

In the following we model the behavior of a network in which the connections not only break after some time, but also get repaired. We assume that the repairing takes some time. Mathematically speaking, the connections can break in each time step with probability $p_\downarrow$, e.g., the breaking is geometrically distributed. If a connection is broken it gets repaired after τ time steps. After this repairing time, the repaired connection can either break directly again with probability $p_\downarrow$ or stay functional with probability $1 - p_\downarrow$. Note that this means that

it is not guaranteed that after τ time steps the connection is functional again; it can well happen that it is broken for 2τ or even more multiples of τ.

We want to calculate the probability that a block of N connections or a network behaves in a certain way in t arbitrarily chosen consecutive time steps. To reach this goal we first calculate the probabilities for a single connection to behave in a certain way in up to three consecutive time steps. Then we show how these probabilities can be used to describe the behavior of a block of N connections and more complex networks.

1. Single connection

We start by calculating all needed probabilities for a single connection.

Proposition 4. The probability for a single connection with failure probability $p_\downarrow$ and repairing time τ to be broken in an arbitrarily chosen time step is given by

$$p_{\text{eff}}^b = \frac{\tau}{1/p_\downarrow - 1 + \tau}. \tag{C1}$$

Proof. Since the breaking of a connection is geometrically distributed, the first break will happen on average in time step $1/p_\downarrow$. Thus, the connection is on average functional for $1/p_\downarrow - 1$ time steps and then broken for another τ time steps. The probability that the connection is broken in an arbitrarily chosen time step is thus

$$p_{\text{eff}}^b = \frac{\tau}{1/p_\downarrow - 1 + \tau} \tag{C2}$$

and the probability that the connection is functional is

$$p_{\text{eff}}^f = \frac{1/p_\downarrow - 1}{1/p_\downarrow - 1 + \tau} = 1 - p_{\text{eff}}^b. \tag{C3}$$

$\blacksquare$

In the next step we want to calculate the probability that a single connection is broken in not only one arbitrarily chosen time step but instead in $1 \leqslant t \leqslant \tau$ consecutive arbitrarily chosen time steps.

Proposition 5. The probability for a single connection with failure probability $p_\downarrow$ and repairing time τ to be broken in
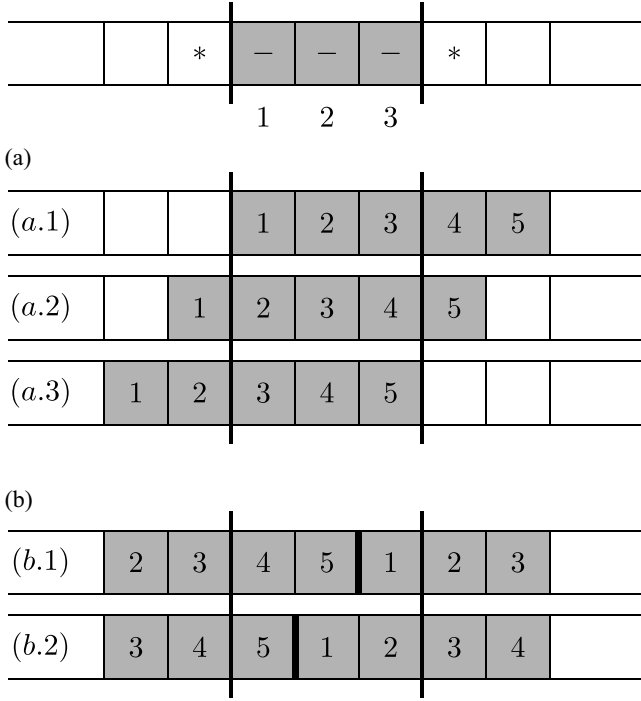
(a)

(b)

FIG. 8. Possible states of a connection with repairing time $\tau = 5$ to be broken in $t = 3$ arbitrarily chosen consecutive time steps. (a) If the first of the consecutive time steps coincides with one of the first $\tau - t + 1 = 3$ broken steps of the connection, the connection is broken throughout the three consecutive time steps. (b) If the first of the consecutive time steps coincides with one of the last $t - 1 = 2$ broken steps of the connection, then the connection has to break again directly after being repaired to remain broken through the three consecutive time steps.

$1 \leqslant t \leqslant \tau$ arbitrarily chosen consecutive time steps is given by

$$m(t) = p_{\text{eff}}^b \left(1 - \frac{t-1}{\tau}(1 - p_\downarrow) \right). \qquad (C4)$$

Proof. The probability for the connection to be broken in t consecutive time steps $m(t)$ can be calculated in a similar way as in Proposition 4 (see also Fig. 8). We saw there that a connection is on average functional for $1/p_\downarrow - 1$ time steps and then broken for another τ time steps. Thus, the first of the t consecutive time steps has to coincide with one of the τ broken steps of the device. If it coincides with one of the first $\tau - t + 1$ broken steps of the device then the device remains surely broken for the following $t - 1$ time steps. If it coincides with one of the $t - 1$ last broken steps of the device then the device has to break again directly after being repaired to stay broken in the remaining $t - 1$ consecutive time steps. This happens with probability $p_\downarrow$. One therefore gets

$$m(t) = \frac{\tau - t + 1}{1/p_\downarrow - 1 + \tau} \times 1 + \frac{t-1}{1/p_\downarrow - 1 + \tau} \times p_\downarrow$$

$$= \frac{\tau}{1/p_\downarrow - 1 + \tau} \left(1 - \frac{(t-1)(1 - p_\downarrow)}{\tau} \right). \qquad (C5)$$
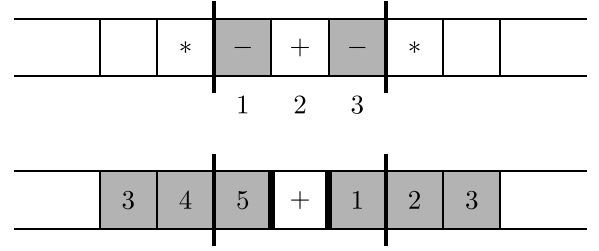
∎

FIG. 9. Possible states of a connection with repairing time $\tau = 5$, which is broken, functional, and broken again in $t = 3$ arbitrarily chosen consecutive time steps. The first of the consecutive time steps has to coincide with the last of the broken steps of the connection. After being repaired, the connection has to stay functional and then break again.

We now use the short notation $+$ or $-$ if the respective system is functional or not functional in a given time step and $*$ if the state of the system is arbitrary or not known. The probability that a connection is broken in three consecutive time steps would then be denoted by $m(3) = p_c^{---}$ and the effective probability for one time step by $p_{\text{eff}}^b = m(1) = p_c^-$. For a single connection all probabilities $p_c^{i_1,\dots,i_t}$ for the behavior $i_1, \dots, i_t$ in t consecutive time steps can be calculated in the same fashion as above by counting all possible states of the connection. One last example for this type of calculation, the probability p_c^{-+-}, is given below, since this probability is needed in the next section treating blocks of N connections.

Proposition 6. The probability for a single connection with failure probability $p_\downarrow$ and repairing time τ to be broken, functional, and broken again in three arbitrarily chosen consecutive time steps is given by

$$p_c^{-+-} = \frac{(1 - p_\downarrow)p_\downarrow}{1/p_\downarrow - 1 + \tau}. \qquad (C6)$$

Proof. The connection is on average functional for $1/p_\downarrow - 1$ time steps and then broken for another τ. For the connection to be broken, functional, and broken again the first of the three consecutive time steps has to coincide with the last time step of the repairing time (see Fig. 9). This happens with probability $\frac{1}{1/p_\downarrow - 1 + \tau}$. After that, the connection stays functional with probability $1 - p_\downarrow$ and breaks again with probability $p_\downarrow$. All in all it holds that

$$p_c^{-+-} = \frac{1}{1/p_\downarrow - 1 + \tau} \times (1 - p_\downarrow) \times p_\downarrow. \qquad (C7)$$

∎

Note that probabilities of the type p_c^{-*-} are given by the sum of all possible cases:

$$p_c^{-*-} = p_c^{-+-} + p_c^{---}. \qquad (C8)$$

2. Block of N connections

To calculate now the probabilities for a block of N connections to be in a certain state in t consecutive time steps, we use two main ingredients. First, we notice that a block is broken if and only if every single connection is broken. So all probabilities for combinations of $-$ and $*$ can be directly

calculated by raising the respective probability for a single connection to the power of N. For example, it holds that

$$p^{---} = (p_c^{---})^N, \quad p^{-*-} = (p_c^{-*-})^N. \tag{C9}$$

Second, we can start computing the probabilities for $t = 1$ arbitrary time step and then recursively calculate the still missing probabilities for more time steps (the ones which contain at least one $+$) by using the marginals. For example, it holds that $p^{+-} + p^{--} = p^{*-} = p^-$. For one time step we get

$$p^+ = 1 - p^-, \tag{C10}$$

for $t = 2$ time steps

$$p^{+-} = p^{-+} = p^- - p^{--}, \tag{C11}$$

$$p^{++} = p^+ - p^{+-}, \tag{C12}$$

and for $t = 3$ time steps

$$p^{+--} = p^{--+} = p^{--} - p^{---}, \tag{C13}$$

$$p^{-+-} = p^{-*-} - p^{---}, \tag{C14}$$

$$p^{-++} = p^{++-} = p^{-+} - p^{+-}, \tag{C15}$$

$$p^{+-+} = p^{+-} - p^{+--}, \tag{C16}$$

$$p^{+++} = p^{++} - p^{++-}. \tag{C17}$$

3. Chain or network

To calculate the probability for a chain or a network to be in a given state in t consecutive time steps we use the approach explained in Appendix B. If the functionality of the system is described by the random variable X we include the time dependence by describing the system in the time steps $1, \ldots, t$ by the random variables $X_1, \ldots, X_t$. The system is then functional in time step k if and only if $\mathbb{1}_{X_k} = 1$. The system being functional in the first step, in an arbitrary state in the second step, and being broken in the third step can be expressed, e.g., by the indicator function

$$\mathbb{1}_S^{+*-} = \mathbb{1}_{X_1} \times 1 \times (1 - \mathbb{1}_{X_3}) \tag{C18}$$

and the according probability can be calculated using

$$p_S^{+*-} = \mathbb{P}(X_1 = 1, X_2 \in \{0, 1\}, X_3 = 0)$$
$$= \mathbb{E}[\mathbb{1}_{X_1} \times 1 \times (1 - \mathbb{1}_{X_3})]. \tag{C19}$$

If $\mathbb{1}_X$ is an expression containing different indicator functions, then each of these needs to get indexed by the time steps. So, e.g., two components in series in time step k are described by $\mathbb{1}_{X_k} = \mathbb{1}_{A_k} \times \mathbb{1}_{B_k}$. The only thing one has to keep in mind is that different components (e.g., A and B) may be independent, but the same component in different time steps A_k and A_j, $j \neq k$, is not. We have to use the probabilities for a single block described in the preceding section. For example, it holds for a block A that

$$\mathbb{E}[\mathbb{1}_{A_1} \mathbb{1}_{A_3}] = p^{+*+} \neq p^+ p^+ = \mathbb{E}[\mathbb{1}_{A_1}]\mathbb{E}[\mathbb{1}_{A_3}]. \tag{C20}$$

APPENDIX D: DESCRIPTION OF THE MODEL AND THE NUMERICAL CALCULATIONS

In the main text we asked whether technical devices are working or not, that is, whether we could in principle establish an entangled connection between two nodes or not. As an application, we simulated the actual generation of entangled links on such not perfectly working repeater chains and networks. In this simulation, to establish an entangled link between two far away parties, we first create shorter entangled links between repeater stations and then connect these by Bell measurements. In our model, we assume deterministic entanglement swapping. Therefore, it is sufficient to create one link on each segment on the way between the two end nodes. We further assume that established links experience decoherence while waiting for other links to get established; this decoherence motivates a potential cutoff after a certain time, as the entanglement in the links becomes too weak or disappears. We are interested in the secret-key rates achievable on a chain or network depending on the functionality of the technical devices. In the following, we discuss details about the simulation program (written in PYTHON) and chosen simulation parameters.

We compute the waiting time as follows. We first simulate the waiting time for each individual connection using Monte Carlo simulation (see, for example, Ref. [71]). In the case of multiplexing, we determine the waiting time of a block by taking the minimum waiting time of all connections associated with that block. The waiting time of the full chain is the maximal waiting time among all blocks. In the network case, the waiting time of the full network is the waiting time of the path which gets established first.

We model memory decoherence as depolarization noise as follows. Each entangled pair is modeled as a Werner state

$$\rho(w) = w|\Psi^-\rangle\langle\Psi^-| + (1 - w)\tfrac{1}{4}, \tag{D1}$$

where w is the visibility (or Werner parameter) and $|\Psi^-\rangle$ is a perfect Bell state. We assume that the sources distribute maximally entangled states, i.e., $w = 1$, but stored entangled states experience decoherence. At time t after establishing the entangled link, the visibility becomes $w(t) = e^{-t/T_{\text{coh}}}$, where T_{coh} is the coherence time of the memories. The fidelity $F = \langle\Psi^-|\rho(w)|\Psi^-\rangle$ is given by $F = \frac{1+3w}{4}$. An entanglement swapping operation using two Werner states $\rho(w_A)$ and $\rho(w_B)$ yields a Werner state $\rho(w_A \times w_B)$.

For the chosen simulation parameters we assume the distance from the source to the repeater to be $L = 100$km. For attenuation losses of 0.2 dB/km, i.e., an attenuation length $L_{\text{att}} \approx 22$km, the probability to generate a link successfully is given by $P_{\text{gen}} = e^{-L/L_{\text{att}}} \approx 0.01$. The length of one time step is limited by $t_{\text{TS}} = \frac{2}{c}L \approx \frac{2}{3} \times 10^{-3}$ s, where c is the speed of light. We assume a memory coherence time of $T_{\text{coh}} = 1$ s $= 1500 t_{\text{TS}}$. (For the motivation for the simulation parameters, see Ref. [60].)

We simulate the behavior of a network and a chain. We consider failure of devices on a different timescale (hours or days) than link generation (seconds). Therefore, we assume that for the time of one entanglement generation attempt the network or the chain has a fixed configuration of working and nonworking devices. The considered network is shown in Fig. 3 and no multiplexing is used. Due to the aging process, some links might not work, so one cannot establish entanglement with them. Using symmetries, we need to consider five different network configurations, which are shown in Fig. 10.
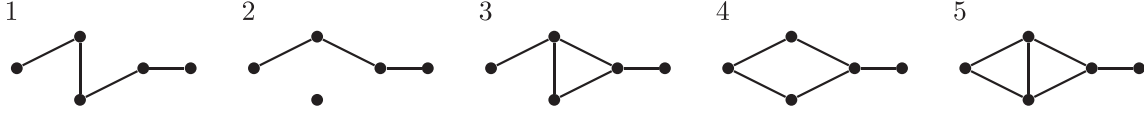
FIG. 10. Possible network configurations allowing for entanglement distribution between the end nodes for the network in the Netherlands (see Fig. 3) up to symmetries.

The chain is of the type shown in Fig. 1. It consists of $M = 6$ segments with a multiplicity of $N = 3$. Due to failures, we might establish entanglement on segments with lower multiplicity. Taking symmetries into account, we have 28 different functional configurations of multiplicities. This number results from taking all combinations of one, two, and three functional connections per edge up to symmetry. For example, the first configurations would be (1,1,1,1,1,1), (1,1,1,1,1,2), (1,1,1,1,1,3), and (1,1,1,1,2,2), where the first three all have one functional connection in the first five edges and one, two, and three connections in the last edge, respectively. The last configuration has one connection in the first four edges and two connections in the last two edges. Note that the second configuration is symmetric to every permutation (1,1,1,1,2,1), (1,1,1,2,1,1), etc., of it.

We modeled 6×10^6 data points for each configuration of the network. Here each data point was generated by a simulation of the process of entanglement generation until success was achieved. Consequently, each data point consisted of a time stamp and a fidelity of the distributed state. From the obtained data we calculated the secret-key rate $R = r/\langle T \rangle$ of the BB84 protocol, which was computed as the fraction of the secret-key fraction r and the average waiting time $\langle T \rangle$. We give here a short overview; for a more detailed discussion see Ref. [32]. The secret-key fraction for a Werner state with visibility w is given by

$$r(w) = \max \left\{ 0, 1 + (1-w) \log_2 \frac{1-w}{2} + (1+w) \log_2 \frac{1+w}{2} \right\}.$$

In order to characterize the effect of different cutoff times, we consider the case that the entanglement generation attempt is terminated after t_{cut} time steps. If there is, after this time, not in every edge an entangled link, then every existing link is erased and a new generation attempt is started. Let T denote the time when every entangled link exists so that the protocol reaches a successful entanglement generation attempt. Then

$$p_{\mathrm{cut}} = \mathbb{P}(T \leqslant t_{\mathrm{cut}})$$

denotes the probability that the entanglement generation is successful during t_{cut} and

$$\frac{\sum_{t=1}^{t_{\mathrm{cut}}} t \, \mathbb{P}(T = t)}{p_{\mathrm{cut}}}$$

is the average time until success during that attempt. The average time for which the cutoff procedure is repeated until the first successful attempt is reached is then geometrically distributed with p_{cut} and given by

$$t_{\mathrm{cut}} \sum_{k=1}^{\infty} k p_{\mathrm{cut}} (1 - p_{\mathrm{cut}})^k = t_{\mathrm{cut}} \frac{1 - p_{\mathrm{cut}}}{p_{\mathrm{cut}}}.$$

All in all, the average waiting time until entanglement generation is given by the sum of the time until the first successful attempt and the waiting time for that success in that attempt:

$$\langle T \rangle = t_{\mathrm{cut}} \frac{1 - p_{\mathrm{cut}}}{p_{\mathrm{cut}}} + \frac{\sum_{t=1}^{t_{\mathrm{cut}}} t \, \mathbb{P}(T = t)}{p_{\mathrm{cut}}}.$$

The resulting end-to-end Werner state has then a visibility parameter W which is the product of the visibilities of the single-connection Werner states in the connected path. Its mean value is given by

$$\langle W \rangle = \frac{\sum_{t=1}^{t_{\mathrm{cut}}} W(t) \mathbb{P}(T = t)}{p_{\mathrm{cut}}}.$$

From the obtained data we can now calculate the secret-key rates R_i for every possible functional configuration i of the network and the chain and every choice of t_{cut}. The average secret-key rate which can be achieved by this protocol on the respective topology is then given by the weighted sum of the different rates where the weights are the probabilities $\mathbb{P}(\text{configuration } i)$ of the different configurations.

The simulation is single threaded but multiple simulations are executed in parallel. The result is obtained by running eight parallel simulations for one to two days on a computer with the following specification: Intel Core i7-4790 CPU with 3.60 GHz running at four cores and eight threads with 16 GB of memory available. The computation is not memory intensive.

[1] N. M. Linke, D. Maslov, M. Roetteler, S. Debnath, C. Figgatt, K. A. Landsman, K. Wright, and C. Monroe, Proc. Natl. Acad. Sci. USA **114**, 3305 (2017).

[2] S. Blinov, B. Wu, and C. Monroe, AVS Quantum Sci. **3**, 033801 (2021).

[3] H. J. Kimble, Nature (London) **453**, 1023 (2008).

[4] S. Wehner, D. Elkouss, and R. Hanson, Science **362**, eaam9288 (2018).

[5] T. J. Proctor, P. A. Knott, and J. A. Dunningham, Phys. Rev. Lett. **120**, 080501 (2018).

[6] X. Guo, C. R. Breum, J. Borregaard, S. Izumi, M. V. Larsen, T. Gehring, M. Christandl, J. S. Neergaard-Nielsen, and U. L. Andersen, Nat. Phys. **16**, 281 (2020).

[7] P. Sekatski, S. Wölk, and W. Dür, Phys. Rev. Res. **2**, 023052 (2020).

[8] P. Komar, E. M. Kessler, M. Bishof, L. Jiang, A. S. Sørensen, J. Ye, and M. D. Lukin, Nat. Phys. **10**, 582 (2014).

[9] S. Barz, E. Kashefi, A. Broadbent, J. F. Fitzsimons, A. Zeilinger, and P. Walther, Science **335**, 303 (2012).

[10] H. J. Briegel, W. Dür, J. I. Cirac, and P. Zoller, Phys. Rev. Lett. **81**, 5932 (1998).

[11] L. M. Duan, M. D. Lukin, J. I. Cirac, and P. Zoller, Nature (London) **414**, 413 (2001).

[12] N. Sangouard, C. Simon, H. de Riedmatten, and N. Gisin, Rev. Mod. Phys. **83**, 33 (2011).

[13] K. Azuma, S. E. Economou, D. Elkouss, P. Hilaire, L. Jiang, H.-K. Lo, and I. Tzitrin, Rev. Mod. Phys. **95**, 045006 (2023).

[14] O. A. Collins, S. D. Jenkins, A. Kuzmich, and T. A. B. Kennedy, Phys. Rev. Lett. **98**, 060502 (2007).

[15] W. J. Munro, K. A. Harrison, A. M. Stephens, S. J. Devitt, and K. Nemoto, Nat. Photonics **4**, 792 (2010).

[16] N. Sinclair, E. Saglamyurek, H. Mallahzadeh, J. A. Slater, M. George, R. Ricken, M. P. Hedges, D. Oblak, C. Simon, W. Sohler, and W. Tittel, Phys. Rev. Lett. **113**, 053603 (2014).

[17] P. Dhara, A. Patil, H. Krovi, and S. Guha, Phys. Rev. A **104**, 052612 (2021).

[18] K. Azuma, K. Tamaki, and H.-K. Lo, Nat. Commun. **6**, 6787 (2015).

[19] J. Borregaard, H. Pichler, T. Schröder, M. D. Lukin, P. Lodahl, and A. S. Sørensen, Phys. Rev. X **10**, 021071 (2020).

[20] S. Muralidharan, L. Li, J. Kim, N. Lütkenhaus, M. D. Lukin, and L. Jiang, Sci. Rep. **6**, 20463 (2016).

[21] S. L. N. Hermans, M. Pompili, H. K. C. Beukers, S. Baier, J. Borregaard, and R. Hanson, Nature (London) **605**, 663 (2022).

[22] J. Yin, Y.-H. Li, S-K. Liao, M. Yang, Y. Cao, L. Zhang, J.-G. Ren, W.-Q. Cai, W.-Y. Liu, S.-L. Li *et al.*, Nature (London) **582**, 501 (2020).

[23] Y. F. Pu, N. Jiang, W. Chang, H. X. Yang, C. Li, and L. M. Duan, Nat. Commun. **8**, 15359 (2017).

[24] J. Sperling, M. Bohmann, W. Vogel, G. Harder, B. Brecht, V. Ansari, and C. Silberhorn, Phys. Rev. Lett. **115**, 023601 (2015).

[25] K. Azuma, S. Bäuml, T. Coopmans, D. Elkouss, and B. Li, AVS Quantum Sci. **3**, 014101 (2021).

[26] L. Praxmeyer, arXiv:1309.3407.

[27] E. Shchukin, F. Schmidt, and P. van Loock, Phys. Rev. A **100**, 032322 (2019).

[28] L. Kamin, E. Shchukin, F. Schmidt, and P. van Loock, Phys. Rev. Res. **5**, 023086 (2023).

[29] S. E. Vinay and P. Kok, Phys. Rev. A **99**, 042313 (2019).

[30] W. Dai and D. Towsley, arXiv:2111.10994.

[31] S. Brand, T. Coopmans, and D. Elkouss, IEEE J. Sel. Areas Commun. **38**, 619 (2020).

[32] B. Li, T. Coopmans, and D. Elkouss, IEEE Trans. Quantum Eng. **2**, 4103015 (2021).

[33] T. Coopmans, S. Brand, and D. Elkouss, Phys. Rev. A **105**, 012608 (2022).

[34] Á. G. Iñesta, G. Vardoyan, L. Scavuzzo, and S. Wehner, npj Quantum Inf. **9**, 46 (2023).

[35] S. Khatri, C. T. Matyas, A. U. Siddiqui, and J. P. Dowling, Phys. Rev. Res. **1**, 023032 (2019).

[36] L. Bugalho, B. C. Coutinho, F. A. Monteiro, and Y. Omar, Quantum **7**, 920 (2023).

[37] B. V. Gnedenko, Y. K. Belyayev, and A. D. Solovyev, *Mathematical Methods of Reliability Theory* (Academic, New York, 2014).

[38] L. A. Gavrilov and N. S. Gavrilova, J. Theor. Biol. **213**, 527 (2001).

[39] I. Bazovsky, *Reliability Theory and Practice* (Dover, New York, 2004).

[40] M. Newman, *Networks* (Oxford University Press, Oxford, 2018).

[41] R. Albert and A.-L. Barabási, Rev. Mod. Phys. **74**, 47 (2002).

[42] B. C. Coutinho, W. J. Munro, K. Nemoto, and Y. Omar, Commun. Phys. **5**, 105 (2022).

[43] A. Strikis, S. C. Benjamin, and B. J. Brown, Phys. Rev. Appl. **19**, 064081 (2023).

[44] J. Rabbie, K. Chakraborty, G. Avis, and S. Wehner, npj Quantum Inf. **8**, 5 (2022).

[45] M. T. Todinov, *Flow Networks* (Elsevier, Amsterdam, 2013).

[46] I. B. Gertsbakh, *Reliability Theory: With Applications to Preventive Maintenance* (Springer Science + Business Media, New York, 2000).

[47] W. Weibull, J. Appl. Mech. **18**, 293 (1951).

[48] W. M. Makeham, Assur. Mag. J. Inst. Actuaries **8**, 301 (1860).

[49] B. Gompertz, Philos. Trans. R. Soc. **115**, 513 (1825).

[50] D. Steinsaltz and S. N. Evans, Theor. Popul. Biol. **65**, 319 (2004).

[51] L. A. Gavrilov and N. S. Gavrilova, *The Biology of Life Span: A Quantitative Approach* (Harwood Academic, New York, 1991).

[52] S. DiAdamo, B. Qi, G. Miller, R. Kompella, and A. Shabani, Phys. Rev. Res. **4**, 043064 (2022).

[53] R. Mandil, S. DiAdamo, B. Qi, and A. Shabani, npj Quantum Inf **9**, 85 (2023).

[54] D. L. Zhou, B. Zeng, Z. Xu, and L. You, Phys. Rev. A **74**, 052110 (2006).

[55] T. Kahle, E. Olbrich, J. Jost, and N. Ay, Phys. Rev. E **79**, 026201 (2009).

[56] T. Galla and O. Gühne, Phys. Rev. E **85**, 046209 (2012).

[57] N. Ay, J. Jost, H. Vân Lê, and L. Schwachhöfer, *Information Geometry*, A Series of Modern Surveys in Mathematics, Vol. 64 (Springer, Cham, 2017).

[58] F Rozpędek, K. D. Goodenough, J. Ribeiro, N. Kalb, V. C. Vivoli, A. Reiserer, R. Hanson, S. Wehner, and D. Elkouss, Quantum Sci. Technol. **3**, 034002 (2018).

[59] F. Rozpędek, R. Yehia, K. Goodenough, M. Ruf, P. C. Humphreys, R. Hanson, S. Wehner, and D. Elkouss, Phys. Rev. A **99**, 052330 (2019).

[60] G. Avis, R. Knegjens, A. S. Sørensen, and S. Wehner, arXiv:2305.09635.

[61] S. Wengerowsky, S. K. Joshi, F. Steinlechner, H. Hübel, and R. Ursin, Nature (London) **564**, 225 (2018).

[62] F. Gu, S. G. Menon, D. Maier, A. Das, T. Chakraborty, W. Tittel, H. Bernien, and J. Borregaard, arXiv:2401.12395.

[63] W. K. Hensinger, S. Olmschenk, D. Stick, D. Hucul, M. Yeo, M. Acton, L. Deslauriers, C. Monroe, and J. Rabchuk, Appl. Phys. Lett. **88**, 034101 (2006).

[64] B. Lekitsch, S. Weidt, A. G. Fowler, K. Mølmer, S. J. Devitt, C. Wunderlich, and W. K. Hensinger, Sci. Adv. **3**, e1601540 (2017).

[65] K. Hansenne, Z.-P. Xu, T. Kraft, and O. Gühne, Nat. Commun. **13**, 496 (2022).

[66] G. Murta, F. Grasselli, H. Kampermann, and D. Bruß, Adv. Quantum Technol. **3**, 2000025 (2020).

[67] W.-C. Yeh, Y.-C. Lin, Y. Y. Chung, and M. Chih, IEEE Trans. Reliab. **59**, 212 (2010).

[68] W. Yeh, Int. J. Syst. Sci. **38**, 87 (2007).

[69] L. Vandré and T. Coopmans, Aging and reliability of quantum networks, https://gitlab.com/alvla/aging-and-reliability-of-quantum-networks (2023).

[70] A. Engel, *Wahrscheinlichkeitsrechnung und Statistik* (Klett, Stuttgart, 1973).

[71] J.-C. Walter and G. Barkema, Physica A **418**, 78 (2015).